Published in final edited form as:
Neuroimage. 2012 January 16; 59(2): 1639–1646. doi:10.1016/j.neuroimage.2011.09.014.

Independent predictors of neuronal adaptation in human primary visual cortex measured with high-gamma activity

Naoyuki Matsuzaki[1], **Tetsuro Nagasawa**[1], **Csaba Juhász**[1,2], **Sandeep Sood**[3], and **Eishi Asano**[1,2,*]

[1]Department of Pediatrics, Children's Hospital of Michigan, Wayne State University, Detroit Medical Center, Detroit, Michigan, 48201, USA.

[2]Department of Neurology, Children's Hospital of Michigan, Wayne State University, Detroit Medical Center, Detroit, Michigan, 48201, USA.

[3]Department of Neurosurgery, Children's Hospital of Michigan, Wayne State University, Detroit Medical Center, Detroit, Michigan, 48201, USA.

Abstract

Neuronal adaptation is defined as a reduced neural response to a repeated stimulus and can be demonstrated by reduced augmentation of event-related gamma activity. Several studies reported that variance in the degree of gamma augmentation could be explained by pre-stimulus low-frequency oscillations. Here, we measured the spatio-temporal characteristics of visually-driven amplitude modulations in human primary visual cortex using intracranial electrocorticography. We determined if interstimulus intervals or pre-stimulus oscillations independently predicted local neuronal adaptation measured with amplitude changes of high-gamma activity at 80–150 Hz. Participants were given repetitive photic stimuli with a flash duration of 20 μsec in each block; the inter-stimulus interval was set constant within each block but different (0.2, 0.5, 1.0 or 2.0 sec) across blocks. Stimuli elicited augmentation of high-gamma activity in the occipital cortex at about 30 to 90 msec, and high-gamma augmentation was most prominent in the medial occipital region. High-gamma augmentation was subsequently followed by lingering beta augmentation at 20–30 Hz and high-gamma attenuation. Neuronal adaptation was demonstrated as a gradual reduction of high-gamma augmentation over trials. Multivariate analysis demonstrated that a larger number of prior stimuli, shorter inter-stimulus interval, and pre-stimulus high-gamma attenuation independently predicted a reduced high-gamma augmentation in a given trial, while pre-stimulus beta amplitude or delta phase had no significant predictive value. Association between pre-stimulus high-gamma attenuation and a reduced neural response suggests that high-gamma attenuation represents a refractory period. The local effects of pre-stimulus beta augmentation and delta phase on neuronal adaptation may be modest in primary visual cortex.

*Corresponding Author: Eishi Asano, MD, PhD, MS (CRDSA), Address: Division of Pediatric Neurology, Children's Hospital of Michigan, Wayne State University. 3901 Beaubien St., Detroit, MI, 48201, USA. Phone: 313-745-5547; FAX: 313-745-0955; eishi@pet.wayne.edu.

Keywords

habituation; sensory gating; repetition suppression; event-related gamma-oscillations; pediatric epilepsy surgery

INTRODUCTION

Neuronal adaptation (also known as repetition suppression or habituation) is defined as a reduced neural response to a repeated stimulus, and the brain is believed to rapidly exert the adaptation process in order to cope with sensory overload and save attention for novel stimuli (Ohzawa et al., 1982; Müller et al., 1999; Grill-Spector et al., 2006). Neuronal adaptation can be demonstrated by (i) relatively reduced augmentation in firing rates, (ii) reduced amplitudes of event-related potentials, and (iii) reduced augmentation of event-related gamma activity at >40 Hz on neurophysiological tools as well as (iv) reduced hemodynamic responses on functional MRI (fMRI) (Henson et al., 2004; Grill-Spector et al., 2006; Privman et al., 2011). Human studies using scalp EEG, magnetoencephalography (MEG) and intracranial electrocorticography (ECoG) showed that the amplitude of event-related potentials and the degree of gamma augmentation driven by repeated visual stimuli was smaller than those driven by the initial stimulus (McDonald et al., 2010; Privman et al., 2011). In these studies, such adaptation effects were significant in the occipital-temporal region (a part of higher-order visual areas) at 150 to 600 msec following the onset of stimulus presentation. A recent ECoG study failed to demonstrate such adaptation effects in the lower-order visual area by measuring event-related potentials or gamma augmentation at <70 Hz (Privman et al., 2011). Since high-gamma amplitudes at >80 Hz are tightly correlated with firing rates (Ray et al., 2008), we hypothesize that *in situ* adaptation effects in lower-order visual cortex can be demonstrated using event-related high-gamma activity at >80 Hz.

In the present study, we studied 13 patients with focal epilepsy who underwent extraoperative ECoG for localization of seizure foci and eloquent cortices; thereby, patients were given repetitive photic stimuli at inter-stimulus intervals ranging from 0.2 to 2.0 sec. We initially assessed the spatio-temporal characteristics of amplitude modulations elicited by photic stimuli at inter-stimulus intervals at 2.0 sec. Thereby, the frequency bands were categorized as follows (Flinker et al., 2010; Fukuda et al., 2010; Nagasawa et al., 2011): (i) high-frequency broadband (160–300 Hz); (ii) high-gamma band (80–150 Hz); (iii) gamma band (40–70 Hz); (iv) $beta_2$ band (20–30 Hz). We are aware that distinction between high-frequency broadband and high-gamma band was arbitrarily defined in the present study and that event-related amplitude augmentation at >80 Hz frequently involve a broad rather than distinct narrow frequency band (Crone et al., 2006).

We determined whether lingering amplitude modulations could be present following high-gamma augmentation but prior to the next visual stimulus. We hypothesized that such lingering oscillatory modulations would include beta augmentation (Tallon-Baudry et al., 2001; Fukuda et al., 2010) and high-gamma attenuation (Haenschel et al., 2000; Asano et al., 2009), and such pre-stimulus oscillatory measures could be candidate predictors of neural adaptation.

Using multivariate statistics on multiple candidate predictors, we analyzed the independent effects of inter-stimulus intervals, the number of prior stimuli, and pre-stimulus local oscillations on the degree of visually-driven high-gamma augmentation and tested the following hypotheses. (i) Photic stimuli with shorter inter-stimulus intervals, compared to those with longer ones, would yield smaller augmentation of high-gamma activity. (ii) The

degree of visually-driven high-gamma augmentation would be gradually reduced over trials. (iii) The amplitude of visually-driven high-gamma activity in a given trial would be small when pre-stimulus $beta_2$ oscillations were still augmented and when pre-stimulus high-gamma activity was attenuated. It has been hypothesized that event-related beta augmentation would represent a neural correlate of short-term memory exerted by the underlying cortex (Tallon-Baudry et al., 1999; 2001) and that high-gamma attenuation following event-related high-gamma augmentation would represent a refractory period (Haenschel et al., 2000; Asano et al., 2009).

We also determined the effect of a phase of pre-stimulus delta wave on visually-driven high-gamma augmentation and tested the following hypothesis. (iv) The phase of pre-stimulus delta-wave would predict the degree of high-gamma augmentation driven by an upcoming visual stimulus, as indicated in a previous study of non-human primates (Lakatos et al., 2008), and such an effect of delta-phase would be independent of the number of prior stimuli as well as pre-stimulus $beta_2$ or high-gamma activities.

METHODS

Patients

The inclusion criteria consisted of: (i) patients with focal epilepsy undergoing extraoperative ECoG recording as a part of presurgical evaluation, (ii) ECoG sampling involving the occipital lobe, and (iii) measurement of ECoG amplitude modulations driven by repetitive photic stimuli as described below. The exclusion criteria consisted of: (i) presence of massive brain malformations which confound the anatomical landmarks for the calcarine sulcus, (ii) visual field deficits detected by confrontation, (iii) history of previous epilepsy surgery, (iv) interictal or ictal epileptiform discharges involving the occipital lobe during photic stimulation, and (v) movement artifacts during photic stimulation. We studied a consecutive series of 13 patients satisfying both inclusion and exclusion criteria (age range: 1 – 21 years; 9 females). The study has been approved by the Institutional Review Board at Wayne State University, and written informed consent was obtained from an adult patient and the guardians of pediatric patients.

Extraoperative video-ECoG recording

For extraoperative ECoG recording, subdural platinum grid electrodes (10 mm intercontact distance, 4 mm diameter; Ad-tech, Racine, WI) were surgically implanted. All electrode plates were stitched to adjacent plates or the edge of dura mater, to avoid movement of subdural electrodes after placement. In all patients, intraoperative pictures were taken with a digital camera before dural closure as well as after re-opening, to confirm the spatial accuracy of electrode display on the 3D brain surface reconstructed from MRI (Nagasawa et al., 2011; Wu et al., 2011). Nonetheless, a minor spatial error in coregistration of MRI and subdural electrodes (LaViolette et al., 2011) could not be ruled out in non-visualized occipital regions in some patients in the present study.

Video-ECoG recordings were obtained using a Nihon Kohden Neurofax 1100A Digital System (Nihon Kohden America Inc, Foothill Ranch, CA, USA). The sampling frequency was 1,000 Hz with the amplifier band pass at 0.08 – 300 Hz. The averaged voltage of ECoG signals derived from the fifth and sixth intracranial electrodes of the ECoG amplifier was used as the original reference. ECoG signals were then re-montaged to a common average reference (Wu et al., 2011). Channels contaminated with large interictal epileptiform discharges or artifacts were visually identified and excluded from the common average reference. No notch filter was used for further analysis. All antiepileptic medications were

discontinued on the day of subdural electrode placement. Electrodes overlying seizure onset zones or MR lesions were excluded from further analysis.

Task: Passive exposure to full-field photic stimulation

None of the patients had a seizure within two hours prior to photic stimulation. Repetitive photic stimuli were given while each patient was unsedated and comfortably lying on the bed in a room with all lights off. Patients were instructed to be relaxed and keep their eyes closed without moving or thinking anything in particular. A total of five patients were awake, while the other eight were asleep during the task. None of the patients had a mixture of awake/sleep states during the task. We used the square-shape xenon photic stimulator LS-703A (Nihon Kohden America Inc), connected to the Digital EEG system via the TTL trigger signal, with a stimulus field size of 13 × 3.5 cm (24.4° × 6.6°), a maximum flash energy of 1.28 J, a flash duration of 20 μsec, and a mean luminance of 30,000 cd/m^2. All patients were given four blocks of full-field stroboscopic flash stimuli at a distance of 30 cm from the closed eyes; each block contained a series of 50 stimuli at a different inter-stimulus interval ranging from 0.2 to 2.0 sec; inter-block interval ranged above 20 sec. The inter-stimulus interval was 0.2 sec in the first block and gradually became longer in seven patients, while it was initially 2.0 sec and gradually became shorter in the remaining six. A previous EEG study showed that the amplitude of visual-evoked potentials did not differ across trials, when stimuli were given with inter-stimulus interval of 12 sec (Janz et al., 2001).

Time-frequency analysis

Using BESA® EEG V.5.1.8 software (BESA GmbH, Gräfelfing, Germany), each ECoG trial was transformed into the time-frequency domain by a complex demodulation technique (Papp and Ktonas, 1977; Hoechstetter et al., 2004). A given ECoG signal was assigned an amplitude (also known as a square root of power) as a function of time and frequency at each trial (Fukuda et al., 2010; Wu et al., 2011). The time-frequency transform was obtained by multiplication of the time-domain signal with a complex exponential, followed by a low-pass filter. The low-pass filter used here was a finite impulse response filter of Gaussian shape, making the complex demodulation effectively equivalent to a Gabor transform. For assessment of signals at 20–300 Hz, the amplitude measure was sampled in steps of 5 msec and 10 Hz. The filter had a full width at half maximum of 2 × 7.9 msec in temporal domain and 2 × 14.2 Hz in frequency domain. The corresponding time-frequency resolution was ±7.9 msec and ±14.2 Hz (defined as the 50% power drop of the finite impulse response filter).

Using ECoG obtained during photic stimulation with an inter-stimulus interval of 2.0 sec, we first determined the percent change in amplitude (averaged across trials) relative to the mean amplitude in a reference period between −25 and −5 msec (i.e.: a period between 5 to 25 msec prior to the stimulus onset). This parameter is commonly termed “event-related synchronization and desynchronization” (Pfurtscheller and Lopes da Silva, 1999) or “temporal spectral evolution” (TSE) (Salmelin and Hari, 1994). In the present study, we did not differentiate between phase-locked and non-phase-locked components (Crone et al., 2006); instead, we measured the total amplitude for assessment of neural responses.

To test for statistical significance for each obtained TSE value, the following statistics was performed using the BESA software (Wu et al., 2011). First, a studentized bootstrap statistics was applied to obtain an uncorrected p-value independently for each time-frequency bin. This test compared the amplitude in each time-frequency bin with the averaged amplitude in the reference time period of the corresponding frequency. In a second step, correction for multiple testing was performed on these uncorrected p-values,

accounting for the fact that TSE values at neighboring time bins are partially dependent. For that purpose, a modification of the correction developed by Simes (1986) was used: for each channel and each frequency, p-values were sorted in ascending order (p_i, i = 1, … , N, where N is the number of time bins in a given frequency band). The maximum index m in the sorted array for which $p_i < \alpha \cdot i/N$ was determined. All TSE values with i<m were considered statistically significant. The corrected significance level α was set to 0.05. In all figures, red color indicates augmentation of amplitude, and blue color attenuation of amplitude in the corresponding time-frequency bin relative to the reference period.

Localization of visually-driven amplitude modulations

We determined what proportions of occipital electrode sites in the following categories exhibited significant visually-driven amplitude augmentation driven by photic stimuli with inter-stimulus interval of 2.0 sec (Figure 1): (i) 'medial occipital region' defined as the medial portion of Brodmann Area 17/18 (N=42 sites in total); (ii) 'polar occipital region' as the polar portion of Brodmann Area 17/18 (N=59 sites); (iii) 'inferior occipital-temporal region' as the inferior portion of Brodmann Area 19/37 (N=56 sites); 'lateral occipital-temporal region' as the lateral portion of Brodmann Area 19/37 (N=65 sites). Our prediction was that the majority of medial occipital sites but only a small subset of lateral occipital sites would show significant high-gamma augmentation. Likewise, we determined what proportions of occipital sites exhibited significant high-gamma attenuation following augmentation driven by photic stimuli with inter-stimulus interval of 2.0 sec.

Assessment of the order of amplitude modulations

We determined whether visually-driven high-gamma augmentation preceded beta augmentation, to confirm that the initial neural responses in the primary visual cortex can be reflected by such high-gamma amplitudes. We also tested whether the percent change of amplitude augmentation differed among four frequency bands. The Friedman test (a non-parametric equivalent of the repeated-measures analysis of variance; ANOVA) was applied to all sites showing significant amplitude augmentations of all four frequency bands, to determine whether any outcome of interest (onset latency and degree of augmentation) differed from others. If the p-value was less than 0.05 on the Friedman test, the Wilcoxon signed rank test was applied as a post hoc test to compare the pairwise latencies/amplitudes.

Assessment of the effects of inter-stimulus intervals, repetition, and pre-stimulus oscillations on neural responses in the primary visual cortex

The aforementioned analysis of oscillatory amplitudes modulated by photic stimuli with inter-stimulus interval of 2.0 sec was expected to localize the occipital sites showing significant amplitude augmentations of all four frequency bands. In these occipital sites, we determined the effects of inter-stimulus intervals, number of prior stimuli and pre-stimulus oscillatory amplitudes on neural responses in the primary visual cortex. Univariate regression analysis was applied to each occipital site to determine the correlation between the maximum absolute high-gamma amplitude within 200 msec following the stimulus ($\boldsymbol{Y_{Max\ high\text{-}gamma}}$) in a given trial and the following predictors: (i) inter-stimulus interval ($\boldsymbol{X_{ISI}}$: ranging from 0.2 to 2.0 sec), (ii) trial number ($\boldsymbol{X_t}$: ranging from 1 to 50), (iii) pre-stimulus $beta_2$ amplitude at −25 to −5 msec relative to the onset of next stimulus ($\boldsymbol{X_{Pre\text{-}beta2}}$), and (iv) pre-stimulus high-gamma amplitude at −25 to −5 msec ($\boldsymbol{X_{Pre\text{-}high\text{-}gamma}}$). Subsequently, multivariate regression analysis was applied to determine the independent effects of these predictors on neural responses in a given trial. A predictor with a mean beta-coefficient different from zero (by one-sample t-test) was considered to be an independent predictor of local neural responses in a given trial.

The univariate regression model tested here is shown below.

$$Y_{Max\ high\text{-}\ gamma} = \beta_0 + \beta_i \cdot X_i$$

(i = pre-stimulus beta$_2$ amplitude, or pre-stimulus high-gamma amplitude)

$$Y_{Max\ high\text{-}\ gamma} = \beta_0 + \beta_{ISI} \cdot log\ (X_{ISI})$$

(ISI = inter-stimulus interval)

$$Y_{Max\ high\text{-}gamma} = \beta_0 + \beta_t \cdot 1/\ X_t$$

(t = trial number)

The multiple regression model tested here is shown below.

$$Y_{Max\ high\text{-}gamma} = \beta_0 + \beta_{ISI} \cdot log\ (X_{ISI}) + \beta_t \cdot 1/X_t + \beta_{Pre\text{-}beta2} \cdot X_{Pre\text{-}beta2} + \beta_{Pre\text{-}high\text{-}gamma} \cdot X_{Pre\text{-}high\text{-}gamma}$$

Assessment of the effect of pre-stimulus delta-phase on neural responses in the primary visual cortex

Using ECoG traces during photic stimulation with inter-stimulus interval of 2.0 sec, we determined the effects of pre-stimulus delta-phase on neural responses in a given trial. Similarly to the above, the time-frequency transformation was performed with a time-frequency sampling of 100 msec and 0.5 Hz. With the filter of a full width at half maximum of 2 × 158 msec in temporal domain and 2 × 0.7 Hz in frequency domain, the corresponding time-frequency resolution was ±158 msec and ±0.7 Hz.

Phase angles were computed in the range between 0° and 360°, where 0° and 360° reflect a peak while 180° reflects a trough of the delta wave. Delta-phase was measured not at the onset but 200 msec prior to the onset of photic stimulation, taking into account the time-frequency resolution. We determined whether the phase of delta-wave at 1 Hz ($X_{Pre\text{-}delta}$) could predict the maximum high-gamma amplitude ($Y_{Max\ highgamma}$) in each trial, using the following univariate and multivariate regression models.

The univariate regression model tested here is shown below.

$$Y_{Max\ high\text{-}gamma} = \beta_0 + \beta_{Pre\text{-}delta} \cdot |sin(X_{Pre\text{-}delta})|$$

(Pre-delta = pre-stimulus delta phase)

The multiple regression model tested here is shown below.

$$Y_{Max\ high\text{-}gamma} = \beta_0 + \beta_t \cdot 1/X_t + \beta_{Pre\text{-}beta} \cdot X_{Pre\text{-}beta} + \beta_{Pre\text{-}high\text{-}gamma} \cdot X_{Pre\text{-}high\text{-}gamma} + \beta_{Pre\text{-}delta} \cdot |\ sin(X_{Pre\text{-}delta})|$$

RESULTS

Amplitude-augmentation elicited by photic stimuli with inter-stimulus of 2.0 sec

Amplitude augmentation occurred at approximately up to 80% of medial occipital sites, 50% of polar occipital, 40% of inferior occipital-temporal, and no more than 10% of lateral occipital-temporal sites (Table 1). The probability of sites showing significant amplitude augmentation differed across the four occipital regions (Yates' $p<0.0001$ on chi-square test). A total of 41 occipital sites (23 medial, 12 polar, 5 inferior and 1 lateral) showed significant amplitude augmentations across frequency bands involving 20–300 Hz. In these occipital sites, augmentations of high-frequency broadband, high-gamma and gamma bands preceded

beta$_2$ augmentation and initially involved the medial occipital region and subsequently involved the surrounding region (Figure 2). Both high-gamma and gamma amplitudes showed larger augmentations compared to high-frequency broadband and beta$_2$ (Figure 3), while there was no significant difference in the degree of amplitude augmentation between high-gamma and gamma bands. Thus, the initial neural responses in the primary visual cortex can be reflected by high-gamma amplitudes.

Amplitude-attenuation elicited by photic stimuli with inter-stimulus interval of 2.0 sec

After high-gamma augmentation subsided, significant high-gamma attenuation was observed (Table 2). High-gamma attenuation involved approximately up to 60% of medial and polar occipital sites, less than 20% of inferior occipital-temporal, and no more than 3% of lateral occipital-temporal sites. The probability of sites showing significant amplitude attenuation differed across the four occipital regions (Yates' $p<0.0001$ on chi-square test).

Effects of inter-stimulus intervals, trial number, and pre-stimulus amplitudes on neural responses

The results of univariate analysis are summarized in Table 3. The inter-stimulus interval was positively correlated with the maximum high-gamma amplitude, suggesting that a shorter inter-stimulus interval elicited reduced neural responses in the primary visual cortex (Figure 4). The data plot suggested that the maximum high-gamma amplitude was reduced over trials in an inverse fashion (Figure 5); neural adaptation was indeed demonstrated using high-gamma amplitude measures. Trial number was inversely correlated with the maximum high-gamma amplitude. Not pre-stimulus beta$_2$-amplitude but pre-stimulus high-gamma amplitude was positively correlated with the maximum high-gamma amplitude in a given trial (Figure 6). Separate analyses of awake and asleep patient groups showed that the maximum high-gamma amplitude in a given trial was positively correlated with inter-stimulus interval and pre-stimulus high-gamma amplitude, inversely correlated with trial number ($p<0.05$) but not correlated with pre-stimulus beta$_2$-amplitude ($p>0.05$).

The multivariate regression model incorporating inter-stimulus interval, trial number, pre-stimulus beta$_2$ amplitude and pre-stimulus high-gamma amplitude could predict the maximum high-gamma amplitude in a given trial (mean r^2: 0.34; 95%CI: 0.29 to 0.39). This indicates that 34% of variance of *in situ* neural responses across trials can be explained by this model. All of these predictors except pre-stimulus beta$_2$ amplitude could independently predict the maximum high-gamma amplitude in a given trial with statistical significance (Table 3).

Effects of pre-stimulus delta-phase on neural responses

The data plot suggested that the maximum high-gamma amplitude was associated with a phase of pre-stimulus delta wave at 1.0 Hz in a sinusoidal manner (Figure 7). When the delta phase at −200 msec was around 90° and 270°, greater maximum high-gamma amplitudes were noted. This observation indicates that neural responses in the primary visual cortex were greater when photic stimulus was given around the peak or trough of delta wave at 1.0 Hz. Univariate regression analysis demonstrated that a sine of pre-stimulus delta phase at 1.0 Hz predicted the maximum high-gamma amplitude in a given trial ($p=0.030$).

The multivariate regression model incorporating trial number, pre-stimulus beta$_2$ amplitude and pre-stimulus high-gamma amplitude, and pre-stimulus delta phase at 1.0 Hz could predict the maximum high-gamma amplitude in a given trial (mean r^2: 0.17; 95%CI: 0.12 to 0.22). In this model, trial number and pre-stimulus high-gamma amplitude turned out to be independent predictors of the maximum high-gamma amplitude, while pre-stimulus beta$_2$ amplitude or delta phase had no independent predictive value (Table 3). This indicates that

pre-stimulus beta$_2$ amplitudes and delta phase had only modest effects on *in situ* neural responses, when the effects of trial number and pre-stimulus high-gamma amplitude were taken into account.

DISCUSSION

Neuronal adaptation in the primary visual cortex measured with high-gamma activity

Using high-fidelity ECoG signals sampled directly from human occipital sites, we demonstrated neural adaptation as reflected by reduced high-gamma augmentation over trials. The effect of such adaptation was stronger when visual stimuli were given with shorter inter-stimulus intervals (such as 0.2 sec). We believe that a good temporal resolution of ECoG-based approach helped in understanding the regional neuronal adaptation elicited by rapidly repeated stimuli. With an inter-stimulus interval of ≤2.0 sec, the degree of neural response elicited by each visual stimulus is difficult to assess using BOLD signals, which reflect changes in regional cerebral blood flow and metabolism occurring several seconds after the given stimulus (Janz et al., 2001).

All participants were in a resting state and stimuli were passively given; thus, the observed adaptation effects were irrelevant to task performance. We attempted to understand the mechanism of such neural adaptation by determining what types of pre-stimulus oscillatory measures independently predicted neural responses in a given trial. We found that pre-stimulus high-gamma attenuation was the only oscillatory measure which could independently predict upcoming neural responses. This observation can be explained by the notion that pre-stimulus high-gamma attenuation represents neuronal fatigue or synaptic depression reflecting a refractory period (Paik et al., 2009). Association between shorter inter-stimulus intervals and more reduced high-gamma augmentation is also consistent with the notion that reduced neural responses were at least partially caused by neuronal fatigue. The effect of adaptation exerted by lower-order visual cortex should be taken into account in studies of neural adaptation in higher-order cortices such as inferior temporal regions, where adaptation via summation of complex mechanisms may be exerted (Summerfield et al., 2008; De Baene and Vogels, 2010).

Higher-order cortices presumably provide an expectation or prediction about an upcoming signal to a lower-order cortex through feedback connections (Roland, 2010). A plausible hypothesis is that such feedback signals would be low-frequency rhythms (Chandrasekaran and Ghazanfar, 2011). A previous human study using ECoG recording showed that beta-oscillations were augmented in both lower and higher visual cortices synchronously, when presented visual objects were memorized for 0.8 to 1.6 sec (Tallon-Baudry et al., 2001). The present study failed to provide evidence that the lower-order visual cortex exhibited pre-stimulus beta$_2$ augmentation predicting upcoming neural responses. This failure might be related to the paradigm used in the present study, where short-term memory function was not required to conduct a task.

The present study also demonstrated that pre-stimulus delta-phase predicted upcoming neural responses, but such a predictive value failed to reach significance when the effects of other predictors such as high-gamma attenuation were taken into account in a multivariate model. The participants were not instructed to predict upcoming visual stimulus in the present study. Thus, our observations are not necessarily contradict to the observations in previous studies of humans and non-human primates using ECoG, which suggested that phase entrainment of delta oscillations mediates the effects of expectation or prediction of upcoming stimulus (Lakatos et al., 2008; Stefanics et al., 2010). Nonetheless, multivariate models taking into account the effects of high-gamma attenuation may be warranted in studies of the effects of delta phases in the future.

Limitations of the present study

The present study failed to determine the minimum inter-stimulus intervals for the primary visual cortex to recover from such a neuronal fatigue; inter-stimulus intervals longer than 2.0 sec were not given to patients in the present study. A study using scalp EEG showed that the amplitude of visual-evoked potentials across trials was stable when checkerboard reversal stimuli were given with inter-stimulus interval of 12 sec (Janz et al., 2001). The present study was not designed to determine the effect of sleep on neuronal adaptation in the primary visual cortex. Further studies using a paired (intra-individual) comparison between awake and sleep states are warranted to determine the effects of states on adaptation.

Highlights

Photic stimuli elicited high-gamma augmentation in human occipital cortex.

High-gamma augmentation in lower-order visual areas was reduced over trials.

Pre-stimulus high-gamma attenuation predicted reduced neural responses.

Pre-stimulus beta-amplitude and delta-phase failed to predict neural responses.

Acknowledgments

This work was supported by NIH grants NS47550 & NS64033 (to E. Asano). We are grateful to Harry T. Chugani, M.D., Robert Rothermel, Ph.D., Carol Pawlak, R.EEG./EP.T., Ruth Roeder, R.N., M.S., Sarah Minarik, R.N., B.S.N., Alanna Carlson, M.A. and the staff of the Division of Electroneurodiagnostics at Children's Hospital of Michigan, Wayne State University for the collaboration and assistance in performing the studies described above.

REFERENCE

Asano E, Nishida M, Fukuda M, Rothermel R, Juhász C, Sood S. Differential visually-induced gamma-oscillations in human cerebral cortex. Neuroimage. 2009; 45:477–489. [PubMed: 19135157]

Chandrasekaran C, Ghazanfar AA. When what you see is not what you hear. Nat Neurosci. 2011; 14:675–676. [PubMed: 21613995]

Crone NE, Sinai A, Korzeniewska A. High-frequency gamma oscillations and human brain mapping with electrocorticography. Prog Brain Res. 2006; 159:275–295. [PubMed: 17071238]

De Baene W, Vogels R. Effects of adaptation on the stimulus selectivity of macaque inferior temporal spiking activity and local field potentials. Cereb Cortex. 2010; 20:2145–2165. [PubMed: 20038542]

Flinker A, Chang EF, Kirsch HE, Barbaro NM, Crone NE, Knight RT. Single-trial speech suppression of auditory cortex activity in humans. J Neurosci. 2010; 30:16643–16650. [PubMed: 21148003]

Fukuda M, Juhász C, Hoechstetter K, Sood S, Asano E. Somatosensory-related gamma-, beta- and alpha-augmentation precedes alpha- and beta-attenuation in humans. Clin Neurophysiol. 2010; 121:366–375. [PubMed: 20075003]

Grill-Spector K, Henson R, Martin A. Repetition and the brain: neural models of stimulus-specific effects. Trends Cogn Sci. 2006; 10:14–23. [PubMed: 16321563]

Haenschel C, Baldeweg T, Croft RJ, Whittington M, Gruzelier J. Gamma and beta frequency oscillations in response to novel auditory stimuli: A comparison of human electroencephalogram (EEG) data with in vitro models. Proc Natl Acad Sci USA. 2000; 97:7645–7650. [PubMed: 10852953]

Henson RN, Rylands A, Ross E, Vuilleumeir P, Rugg MD. The effect of repetition lag on electrophysiological and haemodynamic correlates of visual object priming. Neuroimage. 2004; 21:1674–1689. [PubMed: 15050590]

Hoechstetter K, Bornfleth H, Weckesser D, Ille N, Berg P, Scherg M. BESA source coherence: a new method to study cortical oscillatory coupling. Brain Topogr. 2004; 16:233–238. [PubMed: 15379219]

Janz C, Heinrich SP, Kornmayer J, Bach M, Hennig J. Coupling of neural activity and BOLD fMRI response: new insights by combination of fMRI and VEP experiments in transition from single events to continuous stimulation. Magn Reson Med. 2001; 46:482–486. [PubMed: 11550239]

Lakatos P, Karmos G, Mehta AD, Ulbert I, Schroeder CE. Entrainment of neuronal oscillations as a mechanism of attentional selection. Science. 2008; 320:110–113. [PubMed: 18388295]

LaViolette PS, Rand SD, Ellingson BM, Raghavan M, Lew SM, Schmainda KM, Mueller W. 3D visualization of subdural electrode shift as measured at craniotomy reopening. Epilepsy Res. 2011; 94:102–109. [PubMed: 21334178]

McDonald CR, Thesen T, Carlson C, Blumberg M, Girard HM, Trongnetrpunya A, Sherfey JS, Devinsky O, Kuzniecky R, Dolye WK, Cash SS, Leonard MK, Hagler DJ Jr, Dale AM, Halgren E. Multimodal imaging of repetition priming: Using fMRI, MEG, and intracranial EEG to reveal spatiotemporal profiles of word processing. Neuroimage. 2010; 53:707–717. [PubMed: 20620212]

Müller JR, Metha AB, Krauskopf J, Lennie P. Rapid adaptation in visual cortex to the structure of images. Science. 1999; 285:1405–1408. [PubMed: 10464100]

Nagasawa T, Juhász C, Rothermel R, Hoechstetter K, Sood S, Asano E. Spontaneous and visually driven high-frequency oscillations in the occipital cortex: Intracranial recording in epileptic patients. Hum Brain Mapp. 2011

Ohzawa I, Sclar G, Freeman RD. Contrast gain control in the cat visual cortex. Nature. 1982; 298:266–268. [PubMed: 7088176]

Paik SB, Kumar T, Glaser DA. Spontaneous local gamma oscillation selectively enhances neural network responsiveness. PLoS Comput Biol. 2009; 5:e1000342. [PubMed: 19343222]

Papp N, Ktonas P. Critical evaluation of complex demodulation techniques for the quantification of bioelectrical activity. Biomed Sci Instrum. 1977; 13:135–145. [PubMed: 871500]

Pfurtscheller G, Lopes da Silva FH. Event-related EEG/MEG synchronization and desynchronization: basic principles. Clin Neurophysiol. 1999; 110:1842–1857. [PubMed: 10576479]

Privman E, Fisch L, Neufeld MY, Kramer U, Kipervasser S, Andelman F, Yeshurun Y, Fried I, Malach R. Antagonistic Relationship between Gamma Power and Visual Evoked Potentials Revealed in Human Visual Cortex. Cereb Cortex. 2011; 21:616–624. [PubMed: 20624838]

Ray S, Crone NE, Niebur E, Franaszczuk PJ, Hsiao SS. Neural correlates of high-gamma oscillations (60–200 Hz) in macaque local field potentials and their potential implications in electrocorticography. J Neurosci. 2008; 28:11526–11536. [PubMed: 18987189]

Roland PE. Six principles of visual cortical dynamics. Front Syst Neurosci. 2010; 4:28. [PubMed: 20661451]

Salmelin R, Hari R. Spatiotemporal characteristics of sensorimotor neuromagnetic rhythms related to thumb movement. Neuroscience. 1994; 60:537–550. [PubMed: 8072694]

Simes RJ. An improved Bonferroni procedure for multiple tests of significance. Biometrika. 1986; 73:751–754.

Stefanics G, Hangya B, Hernádi I, Winkler I, Lakatos P, Ulbert I. Phase entrainment of human delta oscillations can mediate the effects of expectation on reaction speed. J Neurosci. 2010; 30:13578–13585. [PubMed: 20943899]

Summerfield C, Trittschuh EH, Monti JM, Mesulam MM, Egner T. Neural repetition suppression reflects fulfilled perceptual expectations. Nat Neurosci. 2008; 11:1004–1006. [PubMed: 19160497]

Tallon-Baudry C, Kreiter A, Bertrand O. Sustained and transient oscillatory responses in the gamma and beta bands in a visual short-term memory task in humans. Vis Neurosci. 1999; 16:449–459. [PubMed: 10349966]

Tallon-Baudry C, Bertrand O, Fischer C. Oscillatory synchrony between human extrastriate areas during visual short-term memory maintenance. J Neurosci. 2001; 21:RC177. [PubMed: 11588207]

Wu H, Nagasawa T, Brown EC, Juhász C, Rothermel R, Hoechstetter K, Shah A, Mittal S, Fuerst D, Sood S, Asano E. Gamma-oscillations modulated by picture naming and word reading: Intracranial recording in epileptic patients. Clin Neurophysiol. 2011

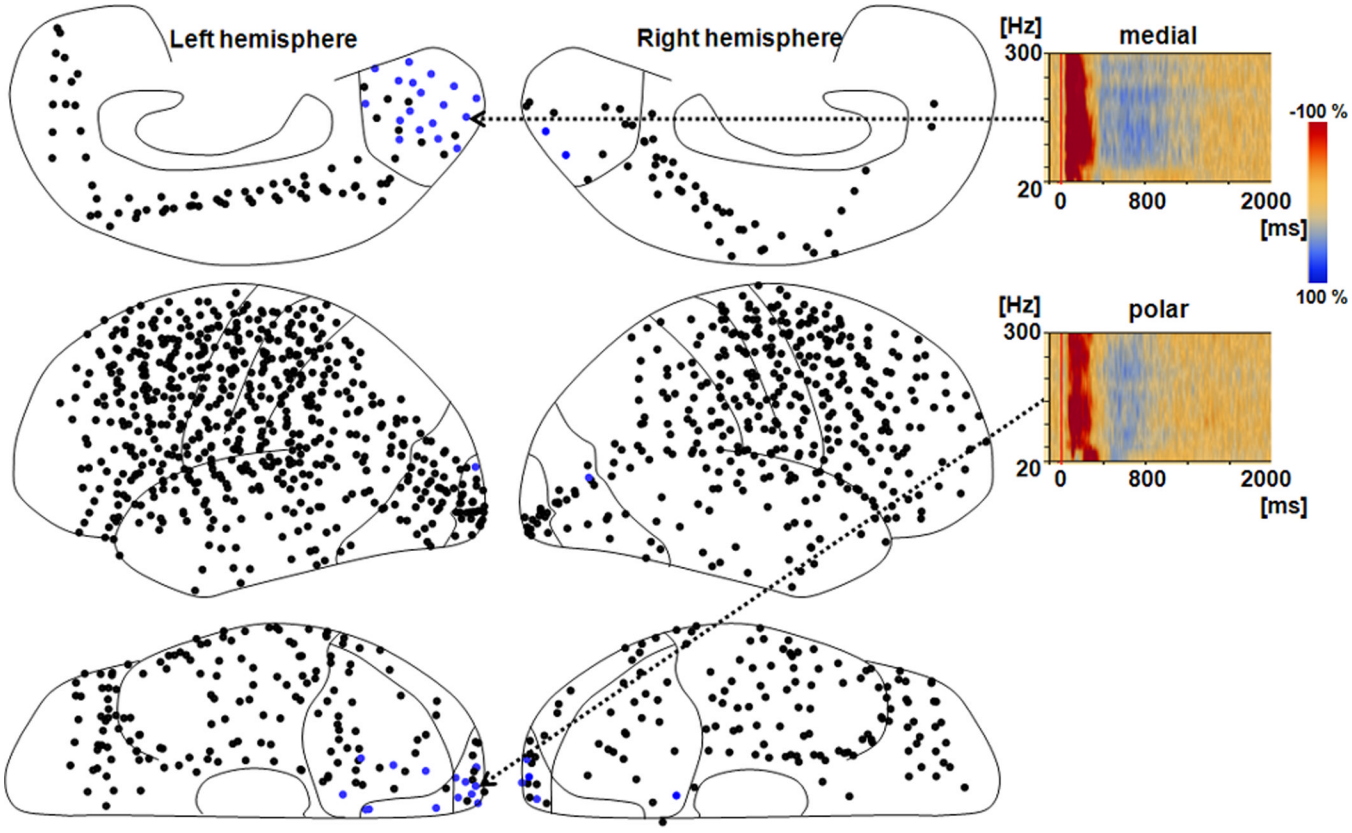

Figure 1. Subdural electrode placement

The locations of subdural electrodes in 13 patients were superimposed on a brain template. A total of 41 electrodes (blue) showed significant amplitude augmentations of high-frequency broadband, high-gamma, gamma and $beta_2$ activities during photic stimulations with inter-stimulus interval of 2.0 sec. Time-frequency matrixes show lingering high-gamma attenuation following high-gamma augmentation. In a polar occipital site, $beta_2$ augmentation followed high-gamma augmentation.

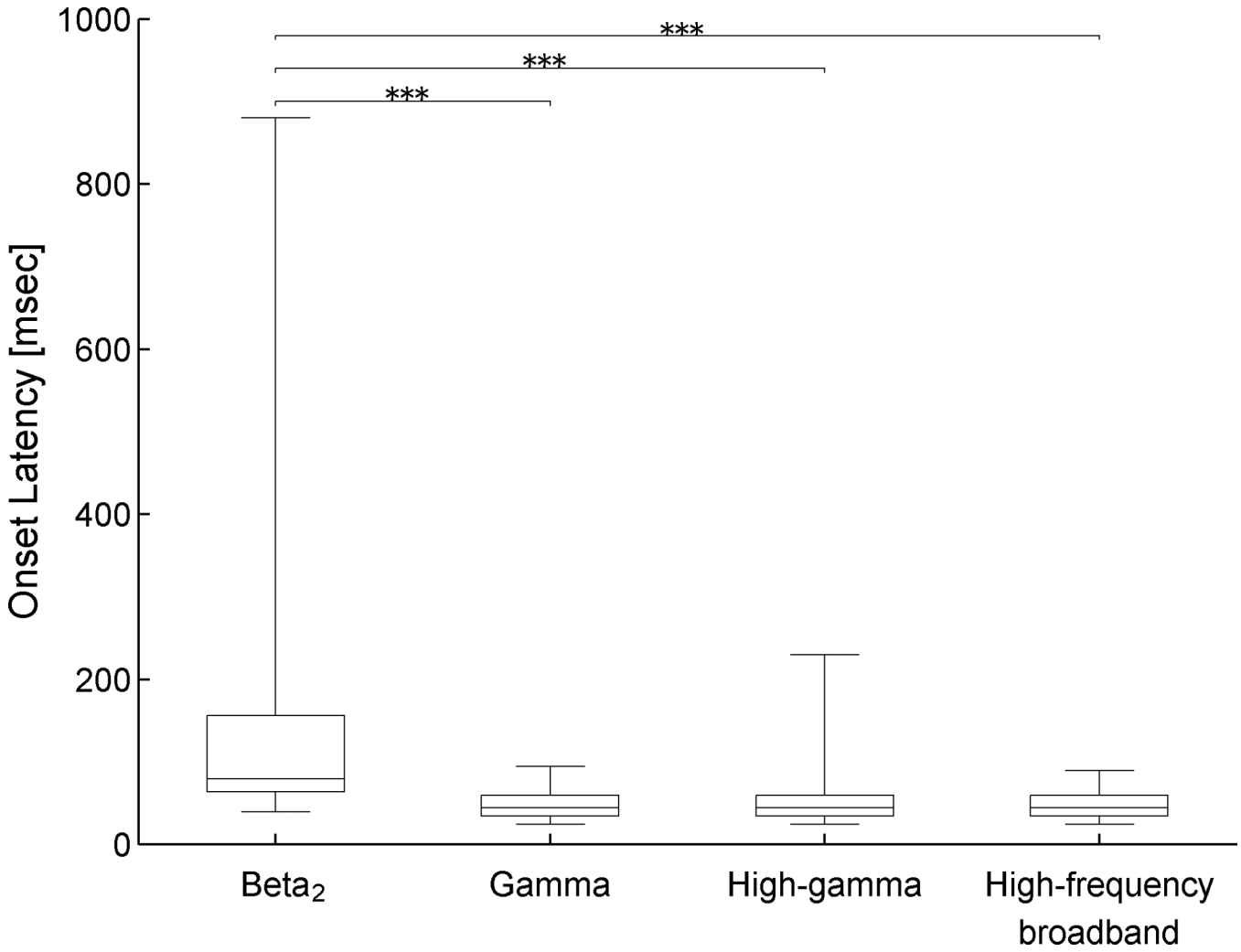

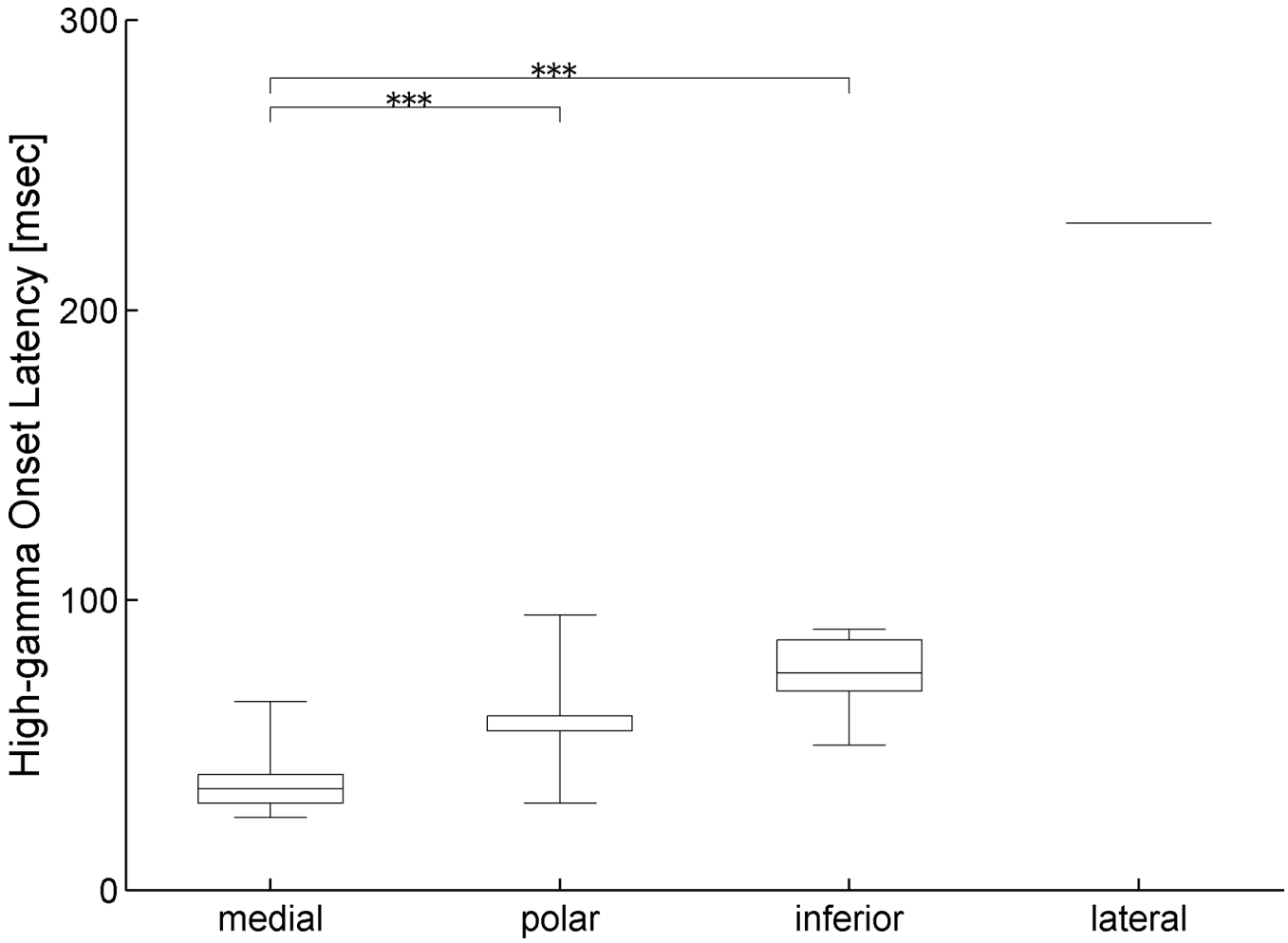

Figure 2. Difference in onset latencies of amplitude augmentations across frequency bands and across sites

(A) The box plots summarize onset latencies across frequency bands. The Friedman test demonstrated that the median onset latency of amplitude augmentation at a frequency band differed from others ($p<0.01$). The Wilcoxon signed rank test demonstrated that the onset latencies of high-frequency broadband (median: 45 msec), high-gamma (median: 45 msec) and gamma augmentations (median: 45 msec) were shorter than that of $beta_2$ augmentation (median: 80 msec). *: $p<0.05$ (after Bonferroni correction). **: $p<0.01$. ***: $p<0.001$.

(B) The box plots summarize onset latencies of high-gamma augmentation across sites. The Kruskal-Wallis test demonstrated that the median onset latency of amplitude augmentation at a region differed from others ($p<0.01$). The medial occipital region had the shortest onset latency of high-gamma augmentation. Difference in onset latency between the medial and lateral occipital sites failed to reach significance on the Mann–Whitney U test, because only a single lateral occipital site was included in the analysis.

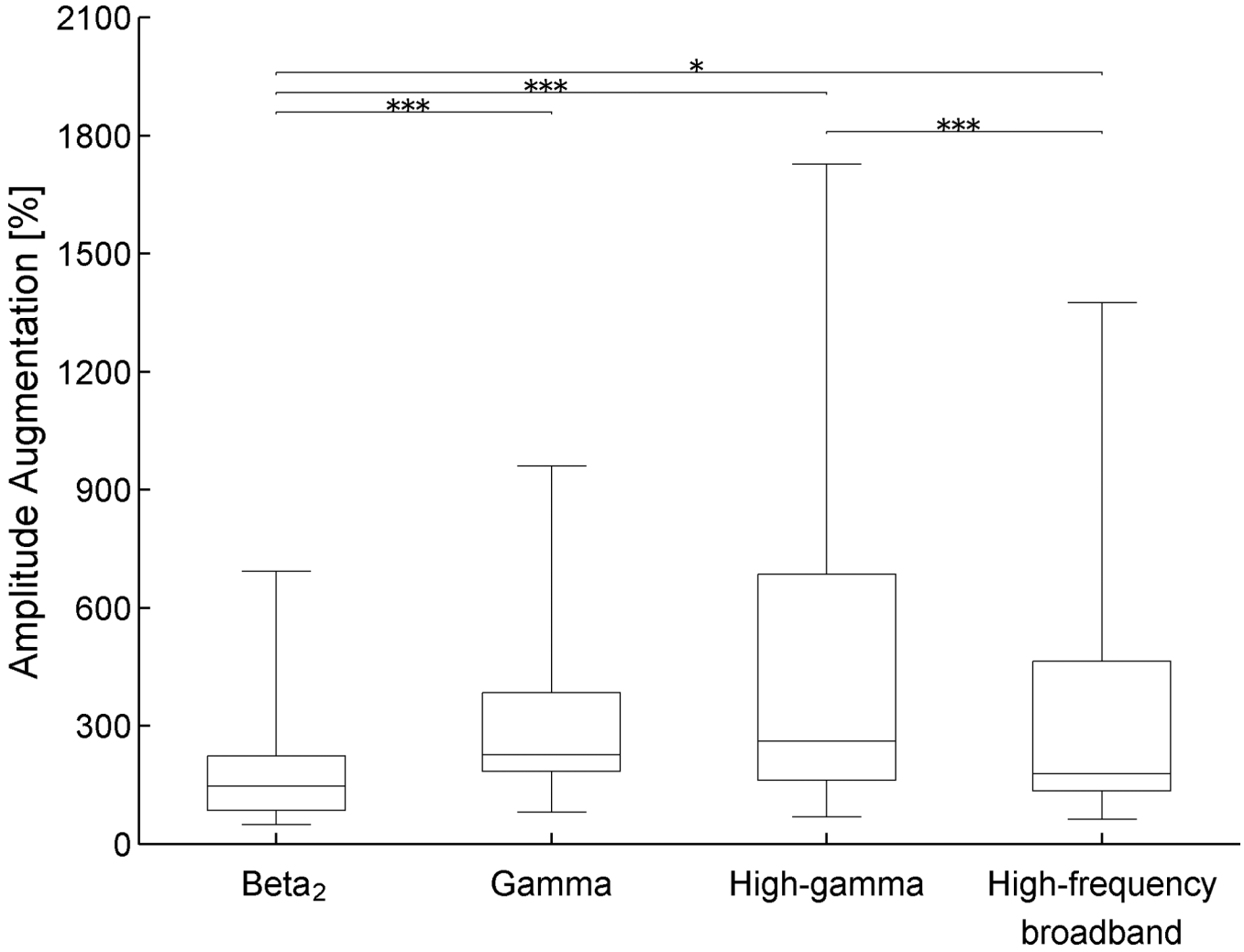

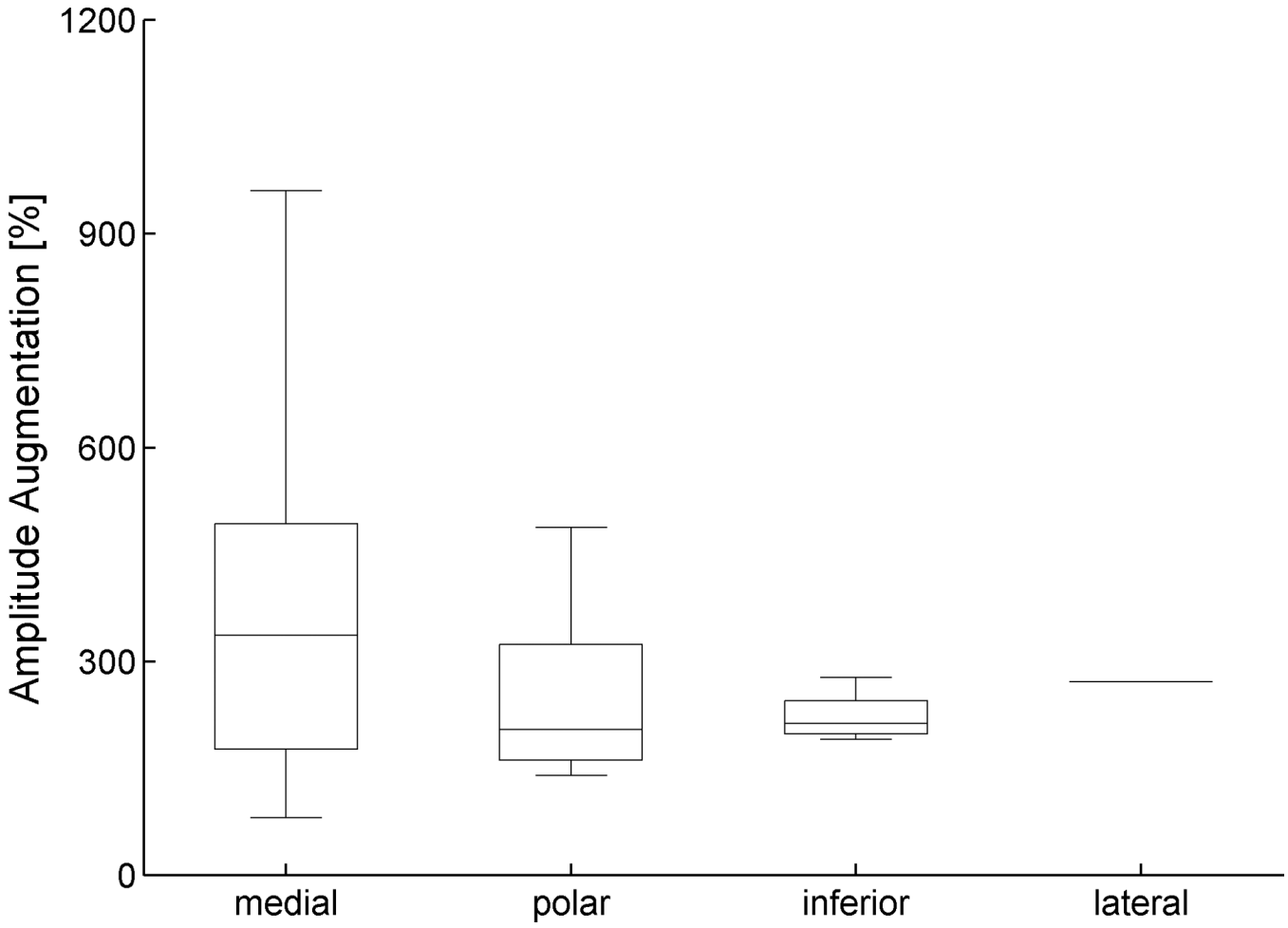

Figure 3. Difference in the degree of amplitude augmentation across frequency bands

(A) The box plots summarize the degree of amplitude augmentations across frequency bands. The Friedman test demonstrated that the percent change of amplitude augmentation at a frequency band differed from others ($p<0.01$). The Wilcoxon signed rank test revealed that the percent change of high-gamma activity (median: +262%) was larger than that of high-frequency broadband activity (median: +179%; $p<0.01$), as well as that of $beta_2$ oscillations (median: +147%; $p<0.01$). There was no significant difference in the degree of amplitude augmentation between high-gamma and gamma (median: +227%) activities. (B) There was no significant difference in the percent change of high-gamma amplitude across the occipital sites.

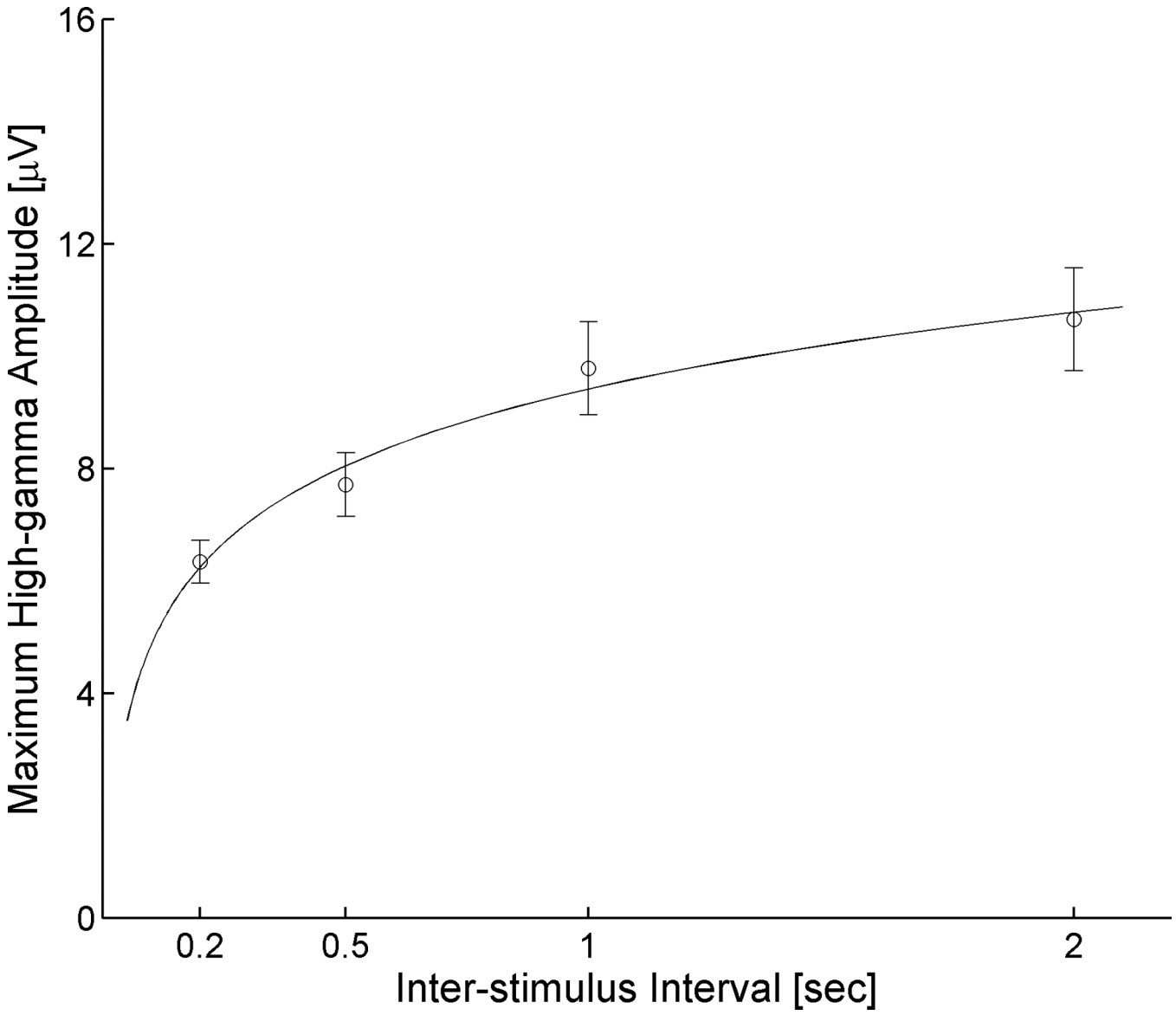

Figure 4. Effects of inter-stimulus intervals on neural responses in the primary visual cortex

A positive correlation was noted between inter-stimulus interval (X-axis) and the maximum high-gamma amplitude within 200 msec following the stimulus in a given trial (Y-axis). Circle: the maximum high-gamma amplitude averaged across trials and occipital sites. Bar: error bar. A regression line: $Y = 9.41 + 4.54 \cdot \log(X)$ is shown.

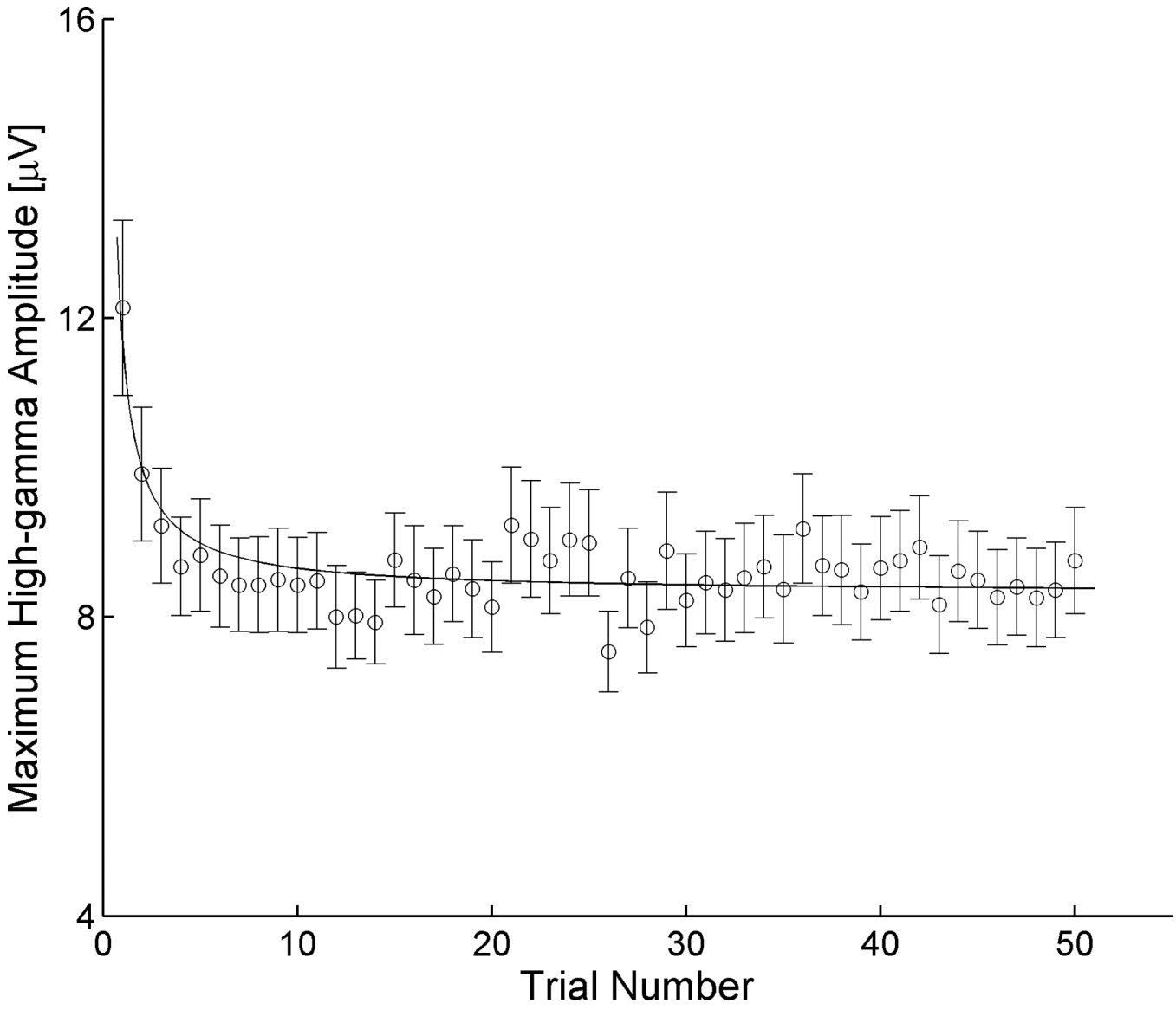

Figure 5. Effects of trial number on neural responses in the primary visual cortex

An inverse correlation was noted between trial number (X-axis) and the maximum absolute high-gamma amplitude within 200 msec following the stimulus in a given trial (Y-axis). Circle: the maximum high-gamma amplitude averaged across occipital sites. Bar: error bar. A regression line: $Y = 8.32 + 3.33 \cdot 1 / X$ is shown.

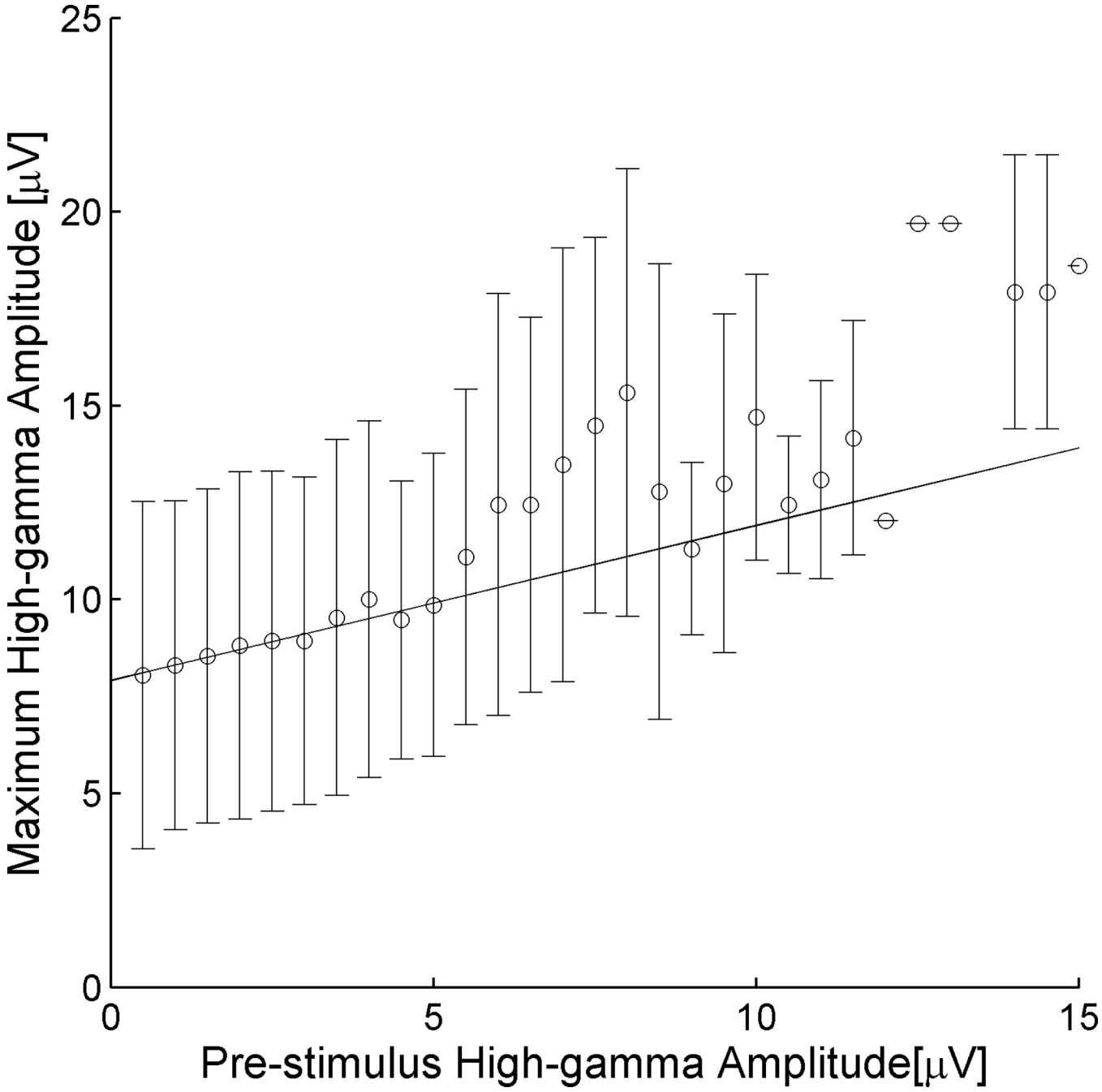

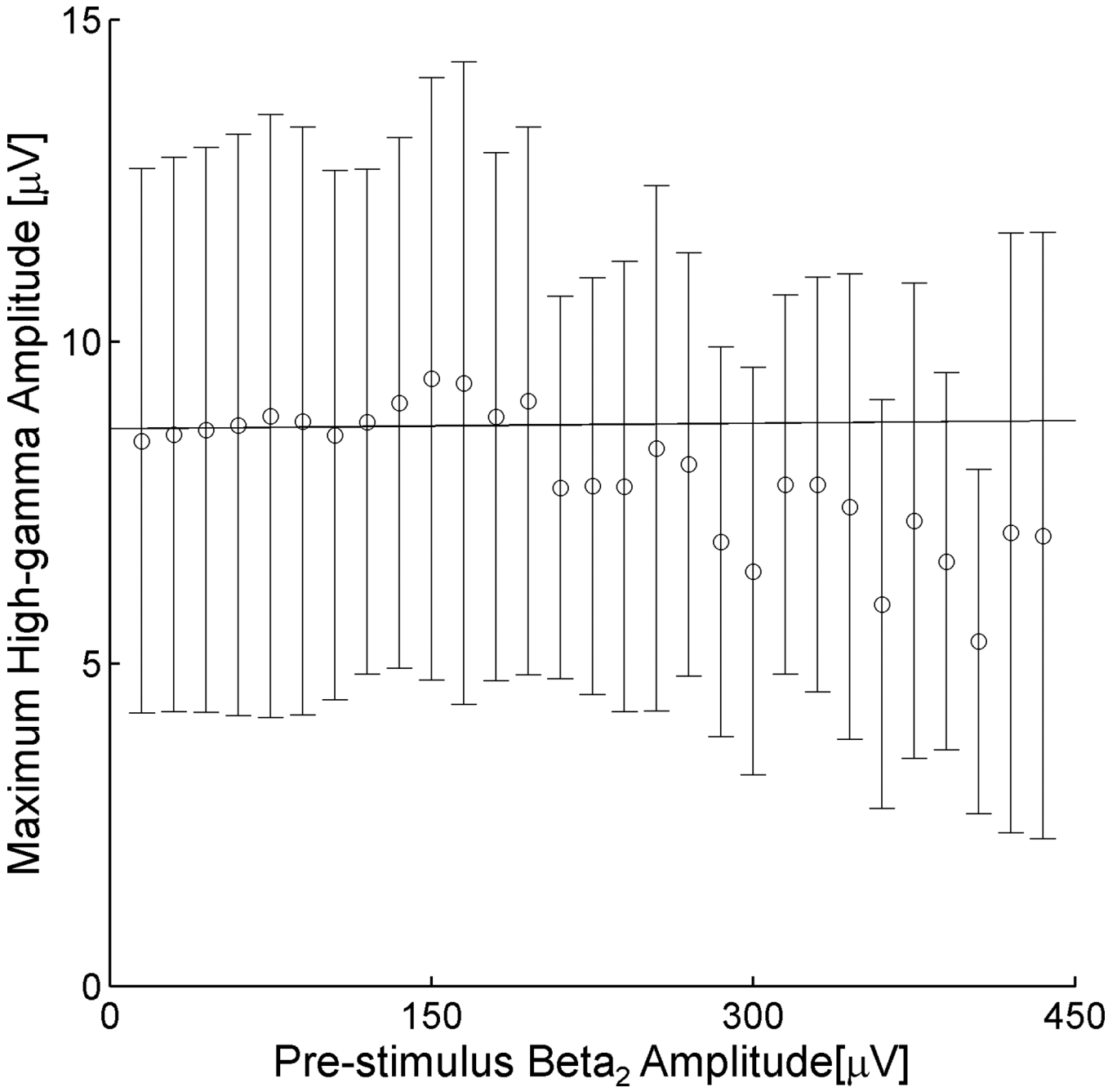

Figure 6. Effects of pre-stimulus amplitudes on neural responses in the primary visual cortex

(A) A positive correlation was noted between pre-stimulus high-gamma amplitude (X-axis) and the maximum absolute high-gamma amplitude within 200 msec following the stimulus in a given trial (Y-axis). Circle: the maximum high-gamma amplitude averaged across a window of 1 μV in X-axis. Bar: standard deviation. A regression line: Y = 7.91 + 0.40 • X is shown.

(B) No linear correlation was noted between pre-stimulus $beta_2$ amplitude (X-axis) and the maximum absolute high-gamma amplitude in a given trial (Y-axis). Circle: the maximum high-gamma amplitude averaged across a window of 30 μV in X-axis. Bar: standard deviation. A regression line: Y = 8.65 + 0.00028 • X is shown.

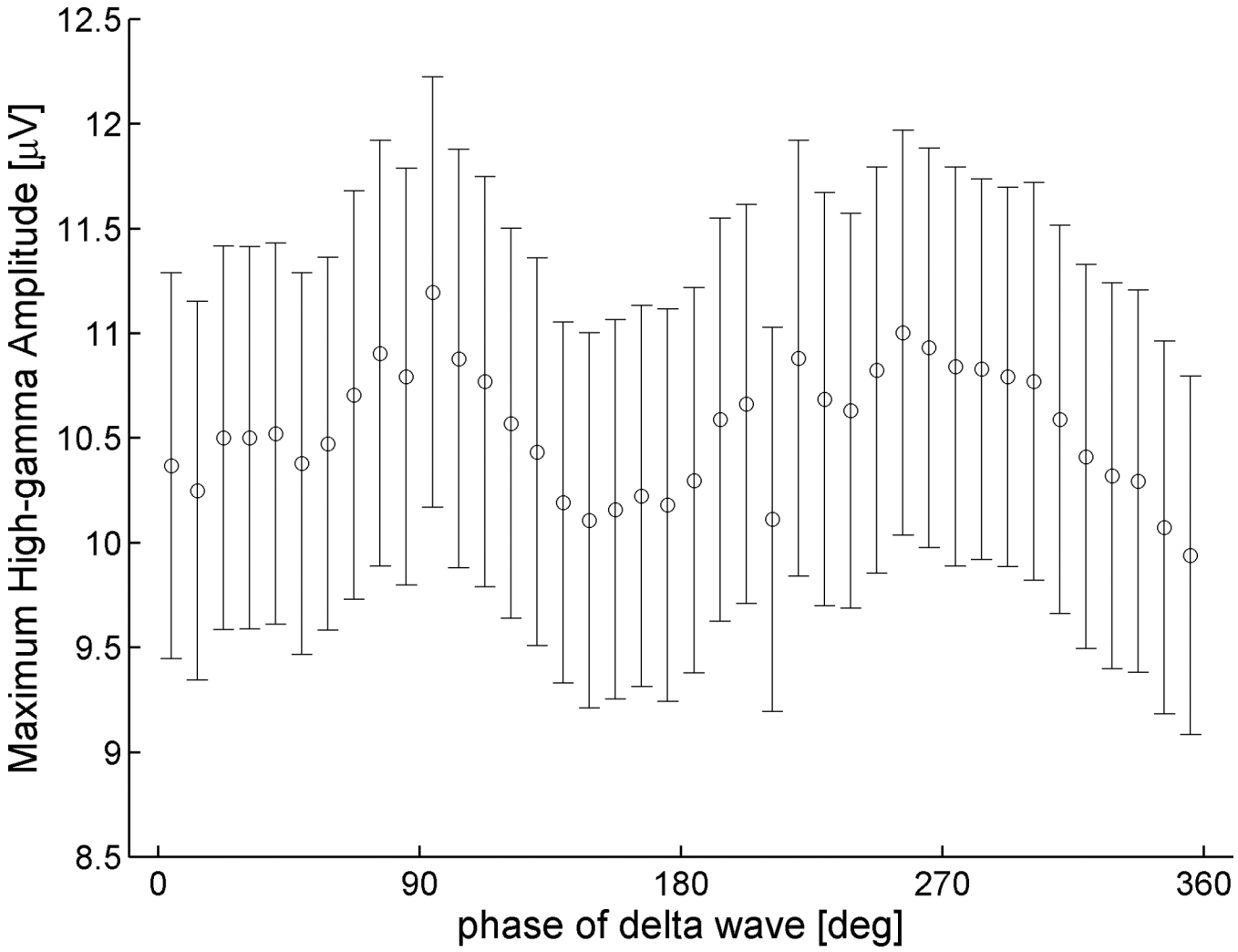

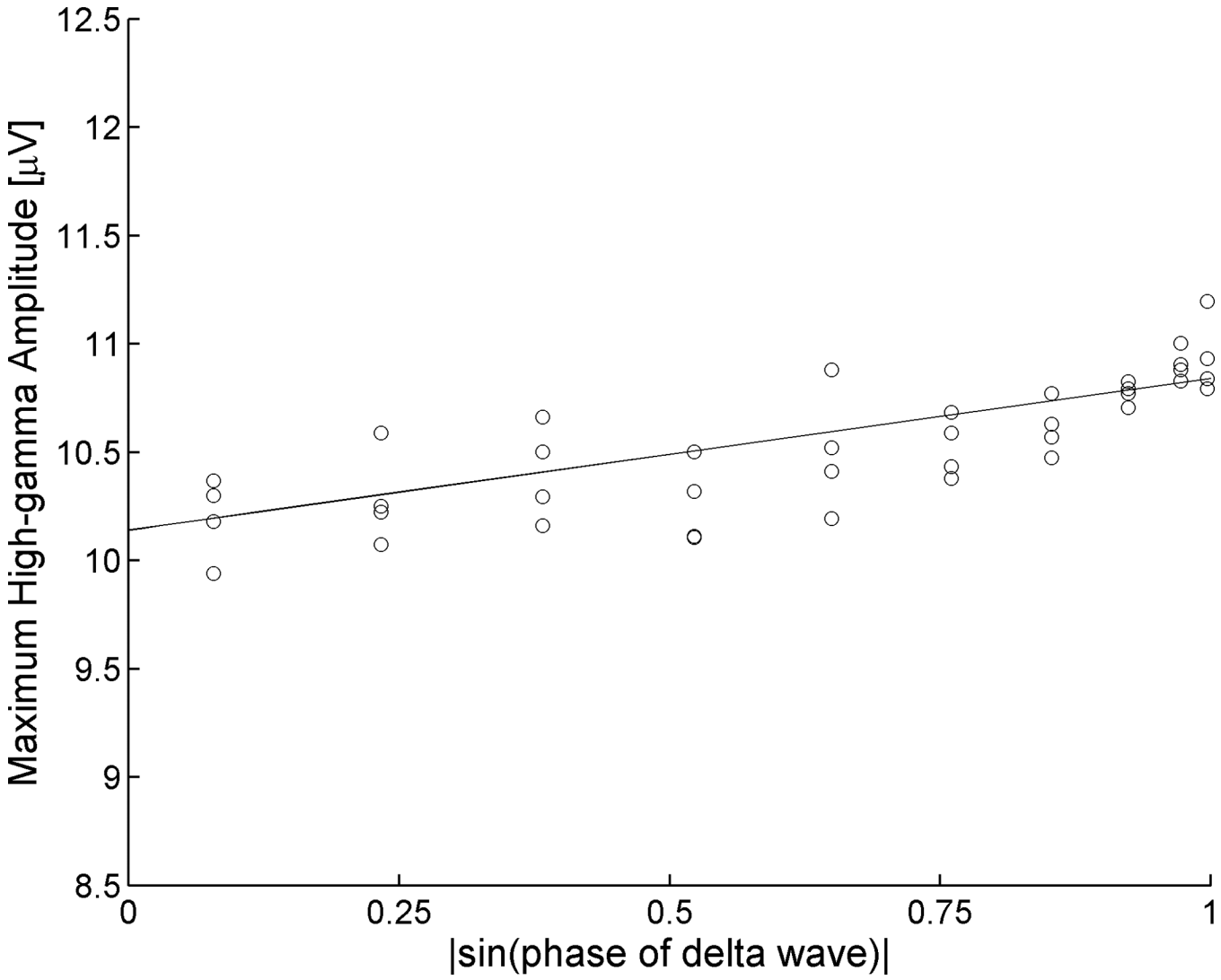

Figure 7. Effects of pre-stimulus delta on neural responses in the primary visual cortex

(A) Pre-stimulus phase of delta wave at 1 Hz (X-axis) predicted the maximum absolute high-gamma amplitude within 200 msec following the stimulus in a given trial (Y-axis). When the phase of delta wave at −200 msec was around 90° and 270°, a greater maximum high-gamma amplitude was noted in a given trial. Circle: the maximum high-gamma amplitude averaged across a window of 45° in X-axis. Bar: error bar.

(B) A linear correlation was noted between a |sines of pre-stimulus delta phase (X-axis)| and the maximum high-gamma amplitude in a given trial (Y-axis). Circle: the maximum high-gamma amplitude averaged across a window of 45° in X-axis. Bar: error bar. A regression line: $Y = 10.14 + 0.70 \cdot X$ is shown.

Table 1

The number of occipital sites showing significant amplitude augmentation

		Number of sites (%) showing significant amplitude augmentation			
Occipital region	**Number of sampled sites**	**High-frequency broadband (160–300 Hz)**	**High-gamma (80–150 Hz)**	**Gamma (40–70 Hz)**	**Beta$_2$ (20–30 Hz)**
Medial occipital	42	33 (79%)	31 (74%)	33 (79%)	31 (74%)
Polar occipital	59	24 (41%)	23 (39%)	20 (34%)	31 (53%)
Inferior occipital-temporal	56	8 (14%)	14 (25%)	10 (18%)	24 (43%)
Lateral occipital-temporal	65	1 (2%)	4 (6%)	2 (3%)	7 (11%)
Whole occipital region	222	66 (30%)	72 (32%)	65 (29%)	93 (42%)

This table shows the number of occipital sites showing significant amplitude augmentation driven by photic stimuli with inter-stimulus interval of 2.0 sec. The probability of sites showing amplitude augmentation differed across four occipital regions (Yates' $p<0.0001$ on chi-square test). The majority of medial occipital sites showed significant amplitude augmentation, while a smaller subset of inferior and lateral occipital-temporal sites showed such augmentation.

Table 2

The number of occipital sites showing significant amplitude attenuation

		Number of sites (%) showing significant amplitude attenuation			
Occipital region	**Number of sampled sites**	**High-frequency broadband (160–300 Hz)**	**High-gamma (80–150 Hz)**	**Gamma (40–70 Hz)**	**$Beta_2$ (20–30 Hz)**
Medial occipital	42	24 (57%)	27 (64%)	21 (50%)	14 (33%)
Polar occipital	59	24 (41%)	34 (58%)	22 (37%)	8 (14%)
Inferior occipital-temporal	56	4 (7%)	9 (16%)	6 (11%)	1 (2%)
Lateral occipital-temporal	65	1 (2%)	2 (3%)	1 (2%)	1 (2%)
Whole occipital region	222	53 (24%)	72 (32%)	50 (23%)	24 (11%)

This table shows the number of occipital sites showing significant amplitude attenuation driven by photic stimuli with inter-stimulus interval of 2.0 sec. The probability of sites showing amplitude attenuation differed across four occipital regions (Yates; $p<0.0001$ on chi-square test). A substantial proportion of medial and polar occipital sites showed significant high-gamma attenuations, while a smaller subset of inferior and lateral occipital-temporal sites showed such attenuations.

Table 3

Beta coefficients in regression models

Predictors	Univariate model	Multivariate model incorporating ISI	Multivariate model incorporating delta-phase
Log (ISI)	4.5** (3.3 to 5.8)	4.5** (3.2 to 5.8)	not incorporated
1 / Trial number	3.3** (2.2 to 4.4)	3.3** (2.3 to 4.4)	4.1** (1.7 to 6.5)
Pre-stimulus $beta_2$ amplitude	0.00028 (−0.003 to 0.004)	−0.001 (−0.003 to 0.0003)	−0.0003 (−0.005 to 0.004)
Pre-stimulus high-gamma amplitude	0.40** (0.18 to 0.63)	0.55** (0.40 to 0.69)	0.44** (0.24 to 0.63)
|sin(delta-phase)|	0.70* (0.07 to 1.3)	not incorporated	0.49 (−0.08 to 1.07)

This table shows a beta co-efficient averaged across 41 occipital sites for a given predictor (with 95% confidence interval).

* $p<0.05$.

** $p<0.01$.

According to the results of univariate analysis, for example, pre-stimulus high-gamma amplitude was positively correlated with the maximum high-gamma amplitude in a given trial and that the beta coefficient was 0.40 on average. This indicates that each 1 μV reduction of pre-stimulus high-gamma amplitude resulted in 0.4 μV reduction of the maximum high-gamma amplitude in a given trial at each site. Inter-stimulus interval (ISI) was not incorporated as a predictor in the multivariate model incorporating delta-phase, since a period shorter than 1 sec cannot contain a single delta wave at 1 Hz.